

# Bright polariton soliton trains in a semiconductor microcavity

M. Sich<sup>1</sup>, F. Fras<sup>1</sup>, J. K. Chana<sup>1</sup>, D. V. Skryabin<sup>2</sup>, A. V. Gorbach<sup>2</sup>, E. A. Cerda-Méndez<sup>3</sup>, K. Biermann<sup>3</sup>, R. Hey<sup>3</sup>, P. V. Santos<sup>3</sup>, M. S. Skolnick<sup>1</sup> and D. N. Krizhanovskii<sup>1</sup>

<sup>1</sup> Department of Physics and Astronomy, University of Sheffield, Sheffield, S3 7RH, UK

<sup>2</sup> Department of Physics, University of Bath, Bath, BA2 7AY, UK

<sup>3</sup> Paul-Drude-Institut für Festkörperelektronik, Hausvogteiplatz 5-7, 10117, Berlin, Germany

Microcavity polaritons are two-dimensional composite bosons arising from strong exciton-photon coupling in semiconductor microcavities. Polariton-polariton interactions enable polariton superfluidity, non-equilibrium condensation as well as formation of dark and bright polariton solitons – localised wavepackets stabilised by nonlinearities. Polariton soliton trains – arrays of consecutive solitons, are an important step towards exploration of fundamental properties of the polariton system such as pattern formation and soliton-soliton interactions. Soliton trains may open a path towards ultrafast all-optical digital information processing.

Solitons form due to the combination of the natural negative effective mass of the lower polariton branch at large  $k$ -vectors (Fig. 1(a)) and polariton-polariton repulsive interactions [1]. For a large pump spot ( $\sim 80 \mu\text{m}$ ), the soliton results from local switching within the bistable area from the lower to the upper state locally in a region of a few microns by a trigger pulsed writing beam (w.b.), as shown on Fig. 1(b).

The size and spacing of solitons inside the train are determined by the polariton healing length ( $\sim 5 \mu\text{m}$ ) – a fundamental characteristic of interparticle interactions in high density states and superfluids. Triggering of the soliton train therefore requires an elongated profile of the w.b. ( $30 \mu\text{m} \times 7 \mu\text{m}$ ). Trains consisting of up to four solitons were reliably observed (Fig. 1(c)). Individual solitons are  $\sim 5 \mu\text{m}$  in size and are equally spaced by  $\sim 5 \mu\text{m}$ .

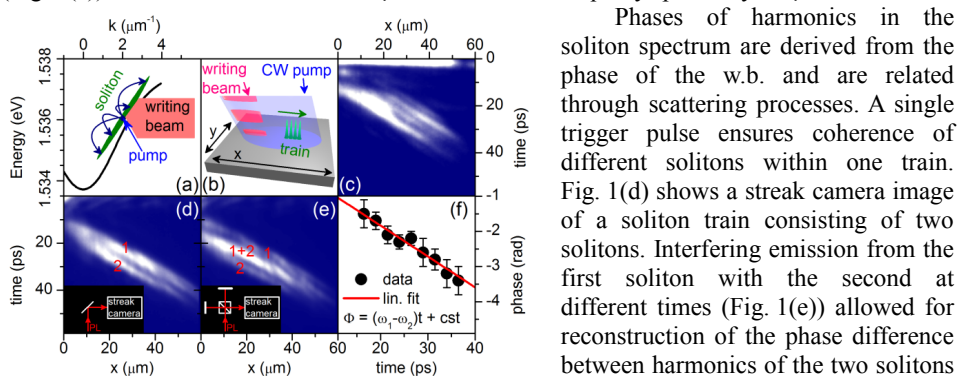


Fig. 1. (a) Dispersion (energy–momentum) diagram of the lower-branch polaritons and schematic representation of the soliton spectrum and excitation scheme. (b) Schematic of soliton train excitation in the microcavity structure. (c) A Streak camera image of a four-soliton train. Streak camera images of a two-soliton train without (d) and with (e) Michelson interferometer in imaging path (see insets). (f) Resolved phase difference between the two solitons, here ‘0’ is arbitrary.

Phases of harmonics in the soliton spectrum are derived from the phase of the w.b. and are related through scattering processes. A single trigger pulse ensures coherence of different solitons within one train. Fig. 1(d) shows a streak camera image of a soliton train consisting of two solitons. Interfering emission from the first soliton with the second at different times (Fig. 1(e)) allowed for reconstruction of the phase difference between harmonics of the two solitons (Fig. 1(f)) as a function of time. The energy difference of  $\sim 50 \mu\text{eV}$  of the detected spectra of the two consecutive solitons is deduced from the linear trend. It results from the complex soliton-soliton interactions which manifest themselves as a redistribution of scattering inside individual solitons.

[1] M. Sich *et al.*, Nature Photon. **6**, 50-55 (2012).

Monday

Tuesday

Wednesday

Thursday

Friday